

REPORT DOCUMENTATION PAGE

Form Approved
OMB No. 0704-0188

Public reporting burden for this collection of information is estimated to average 1 hour per response, including the time for reviewing instructions, searching existing data sources, gathering and maintaining the data needed, and completing and reviewing the collection of information. Send comments regarding this burden estimate or any other aspect of this collection of information, including suggestions for reducing this burden, to Washington Headquarters Services, Directorate for Information Operations and Reports, 1215 Jefferson Davis Highway, Suite 1204, Arlington, VA 22202-4302, and to the Office of Management and Budget, Paperwork Reduction Project (0704-0188), Washington, DC 20503.

1. AGENCY USE ONLY (Leave blank)			2. REPORT DATE May 2004	3. REPORT TYPE AND DATES COVERED Technical Memorandum
4. TITLE AND SUBTITLE Investigation of Gear and Bearing Fatigue Damage Using Debris Particle Distributions			5. FUNDING NUMBERS WBS-22-704-01-03 1L162211A47A	
6. AUTHOR(S) Paula J. Dempsey, David G. Lewicki, and Harry J. Decker			8. PERFORMING ORGANIZATION REPORT NUMBER E-14297	
7. PERFORMING ORGANIZATION NAME(S) AND ADDRESS(ES) National Aeronautics and Space Administration John H. Glenn Research Center at Lewis Field Cleveland, Ohio 44135-3191			10. SPONSORING/MONITORING AGENCY REPORT NUMBER NASA TM-2004-212883 ARL-TR-3133	
9. SPONSORING/MONITORING AGENCY NAME(S) AND ADDRESS(ES) National Aeronautics and Space Administration Washington, DC 20546-0001 and U.S. Army Research Laboratory Adelphi, Maryland 20783-1145				
11. SUPPLEMENTARY NOTES Prepared for the 60th Annual Forum and Technology Display sponsored by the American Helicopter Society, Baltimore, Maryland, June 7-10, 2004. Paula J. Dempsey, NASA Glenn Research Center; and David G. Lewicki and Harry J. Decker, U.S. Army Research Laboratory, NASA Glenn Research Center. Responsible person, Paula J. Dempsey, organization code 5950, 216-433-3398.				
12a. DISTRIBUTION/AVAILABILITY STATEMENT Unclassified - Unlimited Subject Category: 03 Available electronically at http://gltrs.grc.nasa.gov This publication is available from the NASA Center for AeroSpace Information, 301-621-0390.			12b. DISTRIBUTION CODE	
13. ABSTRACT (Maximum 200 words) A diagnostic tool was developed for detecting fatigue damage to spur gears, spiral bevel gears, and rolling element bearings. This diagnostic tool was developed and evaluated experimentally by collecting oil debris data from fatigue tests performed in the NASA Glenn Spur Gear Fatigue Rig, Spiral Bevel Gear Test Facility, and the 500 hp Helicopter Transmission Test Stand. During each test, data from an on-line, in-line, inductance type oil debris sensor was monitored and recorded for the occurrence of pitting damage. Results indicate oil debris alone cannot discriminate between bearing and gear fatigue damage.				
14. SUBJECT TERMS Oil debris; Gears; Bearings; Diagnostics			15. NUMBER OF PAGES 17	
16. PRICE CODE				
17. SECURITY CLASSIFICATION OF REPORT Unclassified	18. SECURITY CLASSIFICATION OF THIS PAGE Unclassified	19. SECURITY CLASSIFICATION OF ABSTRACT Unclassified	20. LIMITATION OF ABSTRACT	



Investigation of Gear and Bearing Fatigue Damage Using Debris Particle Distributions

Paula J. Dempsey
Glenn Research Center, Cleveland, Ohio

David G. Lewicki and Harry J. Decker
U.S. Army Research Laboratory, Glenn Research Center, Cleveland, Ohio

DISTRIBUTION STATEMENT A
Approved for Public Release
Distribution Unlimited

The NASA STI Program Office . . . in Profile

Since its founding, NASA has been dedicated to the advancement of aeronautics and space science. The NASA Scientific and Technical Information (STI) Program Office plays a key part in helping NASA maintain this important role.

The NASA STI Program Office is operated by Langley Research Center, the Lead Center for NASA's scientific and technical information. The NASA STI Program Office provides access to the NASA STI Database, the largest collection of aeronautical and space science STI in the world. The Program Office is also NASA's institutional mechanism for disseminating the results of its research and development activities. These results are published by NASA in the NASA STI Report Series, which includes the following report types:

- **TECHNICAL PUBLICATION.** Reports of completed research or a major significant phase of research that present the results of NASA programs and include extensive data or theoretical analysis. Includes compilations of significant scientific and technical data and information deemed to be of continuing reference value. NASA's counterpart of peer-reviewed formal professional papers but has less stringent limitations on manuscript length and extent of graphic presentations.
- **TECHNICAL MEMORANDUM.** Scientific and technical findings that are preliminary or of specialized interest, e.g., quick release reports, working papers, and bibliographies that contain minimal annotation. Does not contain extensive analysis.
- **CONTRACTOR REPORT.** Scientific and technical findings by NASA-sponsored contractors and grantees.

- **CONFERENCE PUBLICATION.** Collected papers from scientific and technical conferences, symposia, seminars, or other meetings sponsored or cosponsored by NASA.
- **SPECIAL PUBLICATION.** Scientific, technical, or historical information from NASA programs, projects, and missions, often concerned with subjects having substantial public interest.
- **TECHNICAL TRANSLATION.** English-language translations of foreign scientific and technical material pertinent to NASA's mission.

Specialized services that complement the STI Program Office's diverse offerings include creating custom thesauri, building customized databases, organizing and publishing research results . . . even providing videos.

For more information about the NASA STI Program Office, see the following:

- Access the NASA STI Program Home Page at <http://www.sti.nasa.gov>
- E-mail your question via the Internet to help@sti.nasa.gov
- Fax your question to the NASA Access Help Desk at 301-621-0134
- Telephone the NASA Access Help Desk at 301-621-0390
- Write to:
NASA Access Help Desk
NASA Center for AeroSpace Information
7121 Standard Drive
Hanover, MD 21076



Investigation of Gear and Bearing Fatigue Damage Using Debris Particle Distributions

Paula J. Dempsey
Glenn Research Center, Cleveland, Ohio

David G. Lewicki and Harry J. Decker
U.S. Army Research Laboratory, Glenn Research Center, Cleveland, Ohio

Prepared for the
60th Annual Forum and Technology Display
sponsored by the American Helicopter Society
Baltimore, Maryland, June 7–10, 2004

National Aeronautics and
Space Administration

Glenn Research Center

Available from

NASA Center for Aerospace Information
7121 Standard Drive
Hanover, MD 21076

National Technical Information Service
5285 Port Royal Road
Springfield, VA 22100

Available electronically at <http://gltrs.grc.nasa.gov>

Investigation of Gear and Bearing Fatigue Damage Using Debris Particle Distributions

Paula J. Dempsey

National Aeronautics and Space Administration
Glenn Research Center
Cleveland, Ohio 44135

David G. Lewicki and Harry J. Decker
U.S. Army Research Laboratory
Glenn Research Center
Cleveland, Ohio 44135

ABSTRACT

A diagnostic tool was developed for detecting fatigue damage to spur gears, spiral bevel gears, and rolling element bearings. This diagnostic tool was developed and evaluated experimentally by collecting oil debris data from fatigue tests performed in the NASA Glenn Spur Gear Fatigue Rig, Spiral Bevel Gear Test Facility, and the 500hp Helicopter Transmission Test Stand. During each test, data from an on-line, in-line, inductance type oil debris sensor was monitored and recorded for the occurrence of pitting damage. Results indicate oil debris alone cannot discriminate between bearing and gear fatigue damage.

INTRODUCTION

Helicopter transmission diagnostics are of paramount importance to helicopter safety because helicopters depend on the power train for propulsion, lift, and flight maneuvering. In order to predict impending transmission failures, the diagnostic tools used in the health monitoring system must provide real-time performance monitoring of aircraft operating parameters and must be highly reliable to minimize false alarms.

Although the goal in the development of future health monitoring systems (HUMS) is to increase reliability and decrease false alarms, today's HUMS are not yet capable of real-time, on-line, health monitoring. After a flight, recorded vibration data is processed and oil samples collected and analyzed. The current fault detection rate of HUMS by analysis of vibration data is about 70 percent [1]. In addition, false warning rates average 1 per hundred flight hours [2]. Often these systems are complex and require extensive interpretation by trained diagnosticians [3].

Oil analysis, in addition to vibration, is used to indicate transmission health. Gear and bearing fatigue failures in transmissions produce significant wear debris in oil lubrication systems. Several companies manufacture in-line, real-time, inductance type oil debris sensors that measure debris size and count particles [4]. The oil debris sensor used in a previous analysis indicated the debris mass measured by the oil debris monitor showed a significant increase when pitting damage began to occur [5, 6]. This sensor has also been used in aerospace applications for detecting bearing failures in aerospace turbine engines. From the manufacturer's experience with failures in rolling element bearings, an equation was developed to set warning and alarm threshold limits for damaged bearings based on accumulated mass. Regarding its use in helicopter transmissions, a modified version of this sensor has been developed and installed in an engine nose gearbox and is currently being evaluated for an operational AH-64 [7].

Several problems exist with using only oil debris to detect damage of transmission components. The lubrication system of a helicopter transmission system contains relatively large particles (> 100 microns) of debris, generated from a multitude of components with the same composition (low alloy steel) [8]. Often, non-failure debris size and counts may be larger than failure debris. In addition, bearings and gears share common lubrication systems, making it difficult to determine which is failing.

The objective of this paper is to determine if particle size distribution can be used to differentiate between a bearing fatigue failure and a gear fatigue failure, where both share a common lubrication system. Oil debris experimental data was recorded from tests performed in the Spur Gear Fatigue Test Rig, the Spiral Bevel Gear Test Rig, and the 500hp Helicopter Transmission Test Stand at NASA Glenn Research Center.

EXPERIMENTAL

Spur Gear Fatigue Test Rig

Experimental data were recorded from experiments performed in the Spur Gear Fatigue Test Rig [9]. Figure 1 shows the test apparatus in the facility and a photo of the gearbox with the cover removed. Operating on a four square principle, the shafts are coupled together with torque applied by a hydraulic loading mechanism that twists two shafts with respect to one another. The power required to drive the system is only enough to overcome friction losses in the system [10]. The test gears were standard spur gears having 28 teeth, 8.89 cm pitch diameter, and 0.64 cm face width. The test gears are run offset to provide a narrow effective face width to maximize gear contact stress while maintaining an acceptable bending stress. Offset testing also allows four tests on one pair of gears.

Tests were run in a manner that allows pitting fatigue damage to be correlated to the oil debris sensor data. For these tests, run speed was 10,000 RPM and applied torque was 72 and 96 N-m. Prior to collecting test data, the gears were run-in for 1 hour at a torque of 14 N-m. The data measured during this run-in were stored. Then,

the oil debris monitor was reset to zero at the start of the loaded test. Test gears were inspected periodically for damage either manually or using a micro camera connected to a video cassette recorder and monitor. The video inspection did not require gearbox cover removal. When damage was found, the damage was documented and correlated to the test data based on a reading number. In order to document tooth damage, reference marks were made on the driver and driven gears during installation to identify tooth 1. The mating teeth numbers on the driver and driven gears were then numbered from this reference. The gearbox photo in Figure 1 identifies the driver and driven gear with the gearbox cover removed.

Data were collected once per minute from the oil debris, speed and pressure sensors installed on the test rig using the program ALBERT, Ames-Lewis Basic Experimentation in Real Time, co-developed by NASA Glenn and NASA Ames. Reading number is equivalent to minutes and can also be interpreted as mesh cycles equal to reading number times 10^4 . Shaft speed was measured by an optical sensor that creates a pulse signal for each revolution of the shaft. Load pressure was measured using a capacitance type pressure transducer.

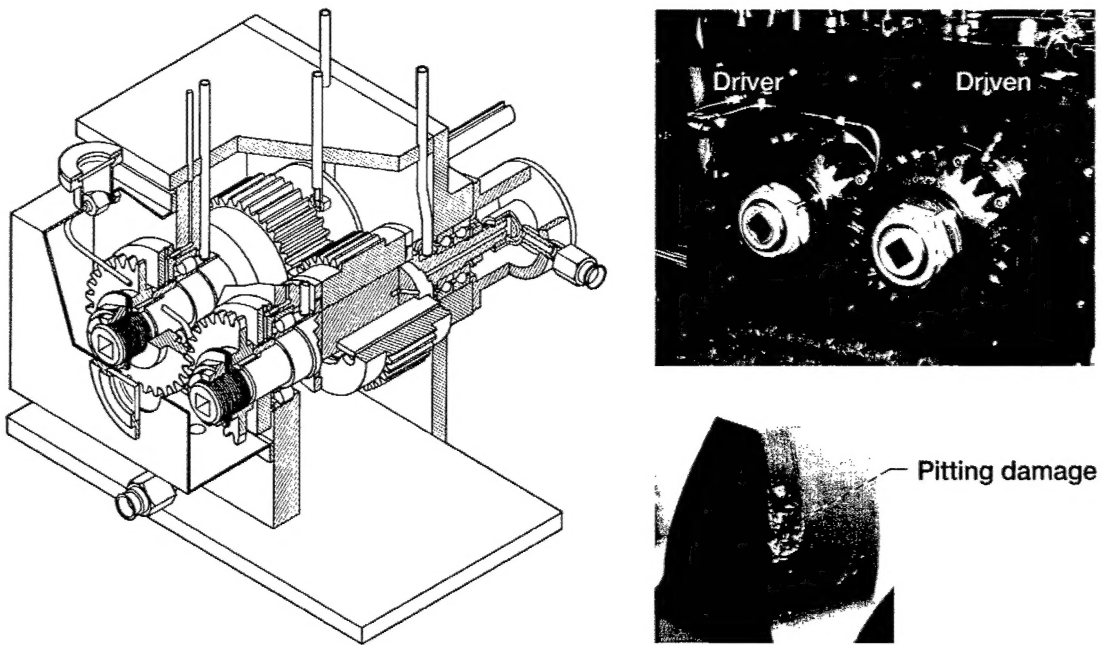


Figure 1.—Spur gear fatigue test rig.

Oil debris data were collected using a commercially available oil debris sensor that measures the change in a magnetic field caused by passage of a metal particle where the amplitude of the sensor output signal is proportional to the particle mass. The sensor counts the number of particles, their approximate size based on user defined particle size ranges, and calculates an accumulated mass [7]. For these experiments, 16 size ranges, referred to as bins, were defined. Based on the bin configuration, the average particle size for each bin is used to calculate the cumulative mass for the experiment. The particle is assumed to be a sphere with a diameter equal to the average particle size. Table 1 lists the 16 particle size ranges and the average particle size used to calculate accumulated mass during spur gear tests. Two filters are located downstream of the oil debris sensor to capture the debris after it is measured by the sensor.

Table 1.—Spur Rig oil debris particle size ranges

Bin	Bin range, μm	Average	Bin	Bin range, μm	Average
1	125–175	150	9	525–575	550
2	175–225	200	10	575–625	600
3	225–275	250	11	625–675	650
4	275–325	300	12	675–725	700
5	325–375	350	13	725–775	750
6	375–425	400	14	775–825	800
7	425–475	450	15	825–900	862.5
8	475–525	500	16	900–1016	958

Although the original intent of testing was the detection of pitting damage on spur and spiral bevel gears, bearing

failures occurred during testing. Pitting is a fatigue failure caused by exceeding the surface fatigue limit of the gear material. Pitting occurs when small pieces of material break off from the gear surface, producing pits on the contacting surfaces [11]. Gears were run until destructive pitting occurred on one or more teeth, where pits are greater than 0.4 mm diameter and cover more than 25 percent of tooth contact area. A gear tooth with the fatigue failure under study is shown in Figure 1. Note the damage is shown on less than half of the tooth due to the offset testing discussed above.

Spiral Bevel Gear Test Facility

Experimental data were recorded from tests performed in the Spiral Bevel Gear Test facility at NASA Glenn Research Center [12, 13]. The Spiral Bevel Gear Test Facility is illustrated in Figure 2. The main purposes of this test rig are to study the effects of gear material, gear tooth design, and lubrication on the fatigue strength of gears. The facility uses a closed loop torque-regenerative system. Two sets of spiral bevel gears can be tested simultaneously. Fatigue tests are performed on aerospace quality gears under varying operating conditions. The 12 tooth pinion and 36 tooth gear have 13.06 cm diametral pitch, 35 degree spiral angle, 2.54 cm face width, 90 degree shaft angle, and 22.5 degree pressure angle. Tests are performed for a specified number of hours or until surface fatigue occurs. The gearbox has a window enabling the test gears to be inspected periodically for damage using a strobe.

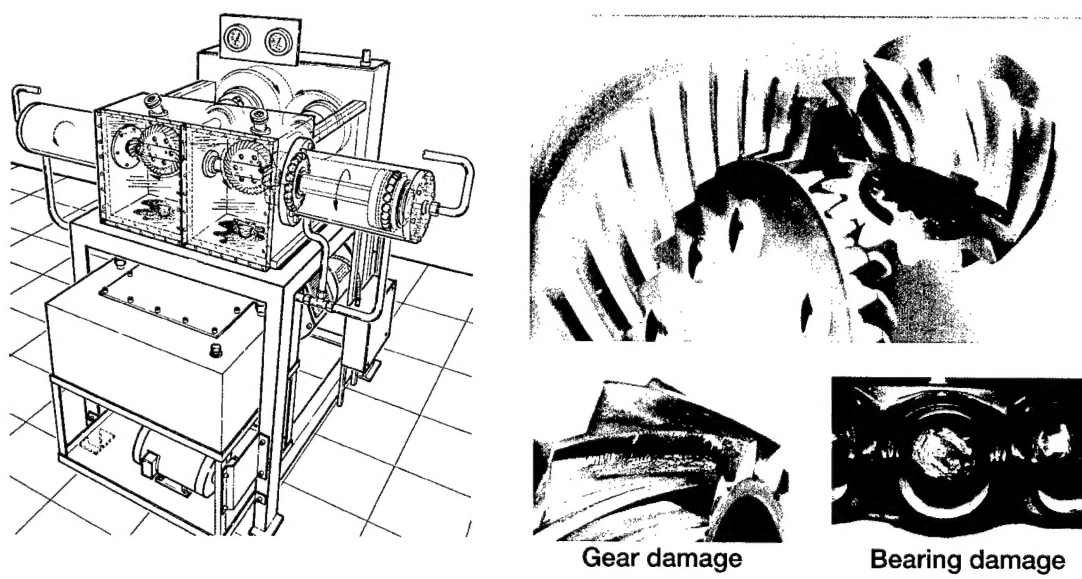


Figure 2.—Spiral bevel gear fatigue rig.

Data were collected once per minute from oil debris, speed and torque sensors installed on the test rig also using ALBERT. Shaft speed was measured by an optical sensor once per each revolution of the test gear shaft. The test pinion had 12 teeth with a shaft speed of 10,200 RPM and the gear had 36 teeth with a shaft speed of 3400 RPM. Torque was measured using a torque meter. Torque on the gear member during testing averaged 849 N-m. Oil debris data were collected using the same type of inductance oil debris sensor as was used for spur gear testing. However, due to the higher oil flow rates in this rig, a larger diameter sensor was required. The smallest particle detected is limited by both sensor size and electrical noise specific to sensor installation location. The voltage output related to the smallest particle measured must be larger than the noise levels in the environment to eliminate false counting in the smallest particle size bin. For these experiments, 14 size ranges were measured, with the smallest particle detected equal to 225 microns. Table 2 lists the 14 particle size ranges and the average particle size used to calculate accumulated mass during spiral bevel gear tests.

Table 2.—Spiral Bevel Rig oil debris particle size ranges

Bin	Bin range, μm	Average	Bin	Bin range, μm	Average
1	225–275	250	8	575–625	600
2	275–325	300	9	625–675	650
3	325–375	350	10	675–725	700
4	375–425	400	11	725–775	750
5	425–475	450	12	775–825	800
6	475–525	500	13	825–900	862.5
7	525–575	550	14	900–1016	958

A representative example of the damage observed on the pinion during spiral bevel gear testing is shown in Figure 2. Pitting damage to the pinion occurred during all experiments. However, during one experiment, bearing damage also occurred. This is also shown in Figure 2.

500-HP Helicopter Transmission Test Stand

Experimental data were recorded from tests performed in the NASA Glenn 500-hp helicopter transmission test stand [14], (Figure 3a). The test stand operates on the closed-loop or torque-regenerative principle. A 149-kW variable-speed direct-current (DC) motor powers the test stand and controls the speed. An 11-kW DC motor provides the torque in the closed loop through use of a magnetic particle clutch and differential gearbox. A mast shaft loading system in the test stand simulates rotor loads imposed on the test transmission output mast shaft. Two vertical load cylinders connected to a loading yoke produce lift loads. One horizontal load cylinder produces bending load.

The test transmission was the OH-58A main rotor transmission (Figure 3b). The design maximum torque and speed for the OH-58A main-rotor transmission is 350 N-m

input torque and 6060 rpm input speed (corresponding to 222 kW). The transmission is a two-stage reduction gearbox. The first stage is a spiral bevel gear set with a 19-tooth pinion that meshes with a 71-tooth gear. Triplex ball bearings and one roller bearing support the bevel-pinion shaft. Duplex ball bearings and one roller bearing support the bevel-gear shaft in an overhung configuration.

A planetary mesh provides the second reduction stage. The bevel-gear shaft is splined to a sun gear shaft. The 27-tooth sun gear drives three or four 35-tooth planet gears, depending on the model. The planet gears mesh with a 99-tooth fixed ring gear splined to the transmission housing. Power is taken out through the planet carrier splined to the output mast shaft. The output shaft is supported on top by a split-inner-race ball bearing and on the bottom by a roller bearing. The overall reduction ratio of the main power train is 17.44:1.

Data were collected from tests performed on the spiral-bevel input pinion [15]. Here, the test transmission was run at 6060 rpm input speed and various levels of torque (280 to 525 N-m) with the goal of initiating and detecting a pinion tooth crack. Oil debris data were collected every 15 seconds using ALBERT and the same type of sensor as in the Spiral Bevel Test Facility. Fourteen size ranges were measured, with the smallest particle detected equal to 250 microns. Table 3 lists the 14 particle size ranges and the average particle size used to calculate accumulated mass.

Table 3.—500hp Test Stand oil debris particle size ranges

Bin	Bin range, μm	Average	Bin	Bin range, μm	Average
1	250–275	263	8	575–625	600
2	275–325	300	9	625–675	650
3	325–375	350	10	675–725	700
4	375–425	400	11	725–775	750
5	425–475	450	12	775–850	813
6	475–525	500	13	850–1000	925
7	525–575	550	14	1000–1016	1008

After 33 hours of run time, the transmission was disassembled and a spalled spiral-bevel gear duplex ball bearing was found (Figures 3b and 3c). A new bearing was installed and the transmission was cleaned and re-assembled. After an additional 39 hours of run time, the transmission was disassembled and a spalled spiral-bevel pinion triplex ball bearing was found (Figures 3b and 3d).

RESULTS AND DISCUSSION

The analysis discussed in this section is based on data collected during 17 experiments in the Spur Gear Fatigue Test Rig, 6 in the Spiral Bevel Gear Test facility, and 2 in the 500hp Transmission Test Stand. The data collected from the Spur Gear Fatigue Rig will be discussed first.

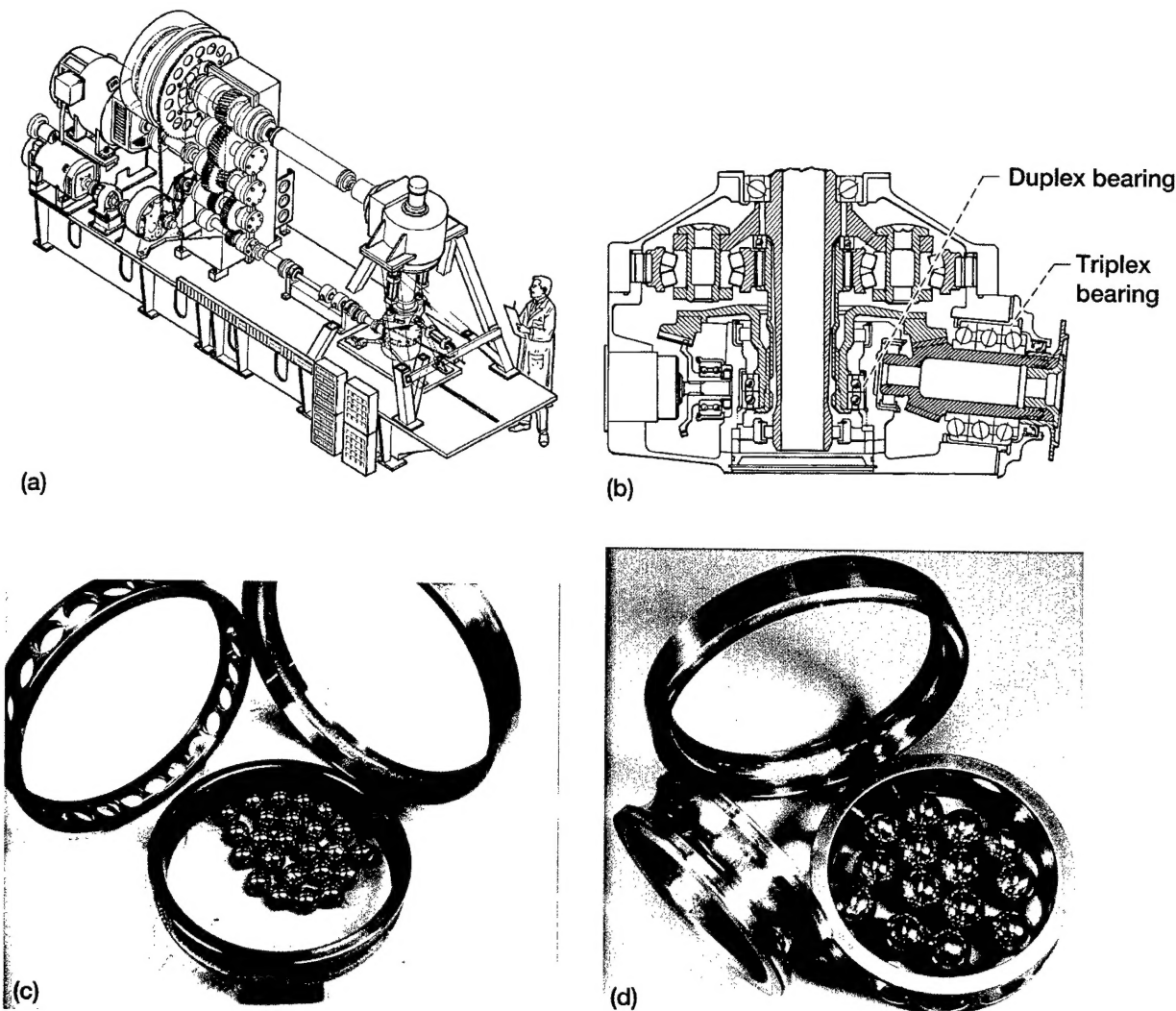


Figure 3.—500 hp helicopter transmission test stand. (a) Rig schematic. (b) OH-58C main rotor transmission. (c) Failed spiral-bevel gear duplex ball bearing. (d) Failed spiral-bevel pinion triplex ball bearing.

Table 4.—Spur Rig Experiments with Gear Pitting Damage

Exp.	Rdg Prior to Damage	Mass (mg)	Counts	Rdg With Damage	Mass (mg)	Counts	Final Rdg with Damage	Mass (mg)	Counts
1	10622	12.5	86	14369	15.5	107	15136	36.1	211
2	1573	3.3	45	2199	8.9	78	2444	26.3	129
3	N/A	N/A	N/A	2669	8.7	64	3029	14.1	117
4	518	9.5	67	2065	12.2	101	4863	26.3	221
5	N/A	N/A	N/A	2566	8.1	97	4425	11.5	160
6	9328	12.0	175	12061	14.6	215	12368	23.1	271
7	N/A	N/A	N/A	N/A	N/A	N/A	13716	3.4	30
8	N/A	N/A	N/A	5181	6.012	63	5314	19.1	132

Spur Gear Fatigue Test Rig

For Experiments 1 through 6, gear tooth pitting damage resulted from the tests and the video inspection system was used. For Experiments 7 and 8, gear tooth pitting damage also resulted from the tests, but visual inspection was performed. For Experiments 9-17, no gear tooth damage was observed for the tests. Table 4 lists the reading numbers

when inspection was performed prior to damage being observed, the reading number when damage was first observed, and the final reading number when the test ended with the corresponding oil debris mass and particle counts at each reading. As can be seen from this table, the amount of mass and the counts varied significantly for each experiment. Note that readings were taken once per minute, and can be interpreted as minutes.

The number of readings, oil debris mass and particle counts for Experiments 9-17, when no damage was observed, are listed in Table 5. At the completion of Experiment 10, 5.5mg of debris was measured, yet no damage occurred. This is more than the debris measured during Experiment 7 (3.381 mg) when initial pitting was observed, due to operational conditions. This and observations made from the data collected during experiments when damage occurred made it obvious that simple linear correlations could not be used to obtain the features for damage levels from the oil debris data.

Table 5.—Spur Rig Experiments without Damage

Exp.	Final Rdg	Mass (mg)	Counts
9	29866	2.4	18
10	20452	5.5	46
11	204	0.4	4
12	15654	2.3	26
13	25259	3.2	47
14	5322	0.00	0
15	21016	0.13	4
16	380	0.10	3
17	21066	0.06	1

Initial analysis of the spur rig Experiments 1 through 6 employed a technique for detecting wear conditions in gear systems by applying statistical distribution methods to particles collected from lubrication systems where the wear activity was determined by the calculated size distribution characteristics [16]. This technique was applied to data sampled off-line. In order to apply this technique to on-line oil debris data, the calculations were made per reading using the average particle size for each bin. Mean particle size, relative kurtosis, and relative skewness were calculated and plotted. From this data, a consistent feature that showed an increase in value as wear occurred was not observed. For

this reason, damage levels using fuzzy logic membership functions using the accumulated debris mass were defined for detecting gear pitting fatigue damage [17]. Additional experiments were performed in the Spur Gear Fatigue Test Rig and have shown accumulated mass is a good predictor of pitting damage on spur gears [18].

Figures 4, 5 and 6 are histograms of the number of particles for each average particle size diameter for Experiments 1 through 17. Figure 4 is the data before damage was observed. Figure 5 is the data after pitting damage was observed. The particle counts increased as damage occurred, and particles were detected in more size ranges. However, the distribution was very similar before and after damage. Figure 6 shows the data collected during experiments without damage. The particle size distribution of the debris is also very similar to the other two figures.

In order to demonstrate this similarity, the mean particle size was calculated for the spur rig experiments prior to, and after damage occurred. Mean particle size was calculated by

$$mps = \sum_{j=1}^N d_j P[d_j]$$

where

d_j = average bin size diameter

N = number of bins

$P[d_j]$ = number of particles per average bin size per reading/total number of particles per reading.

Results of this calculation are shown in Table 6. From this data, it is clear that this statistical parameter, mean particle size, does not vary significantly prior to and after damage has occurred, and should not be used as the feature to indicate gear damage.

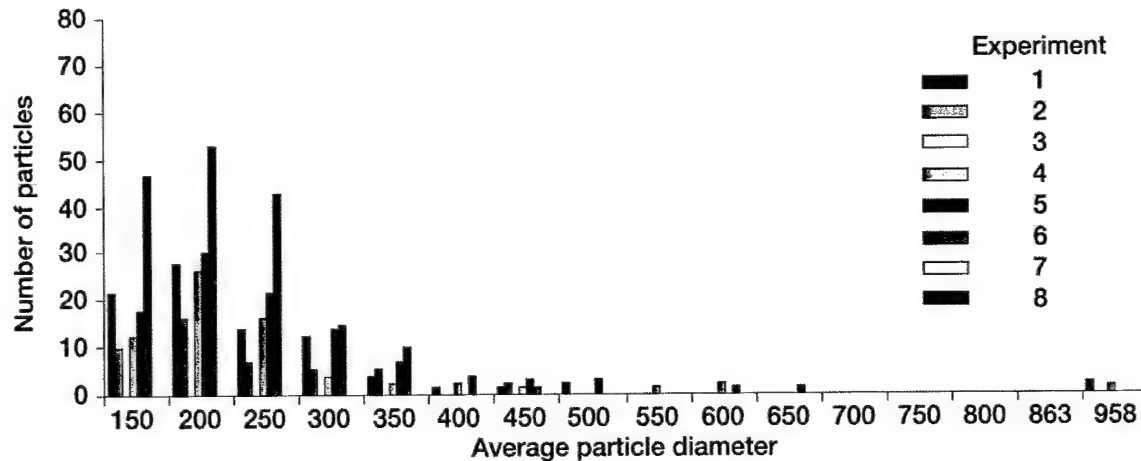


Figure 4.—Spur rig experiments with damage, prior to damage observed.

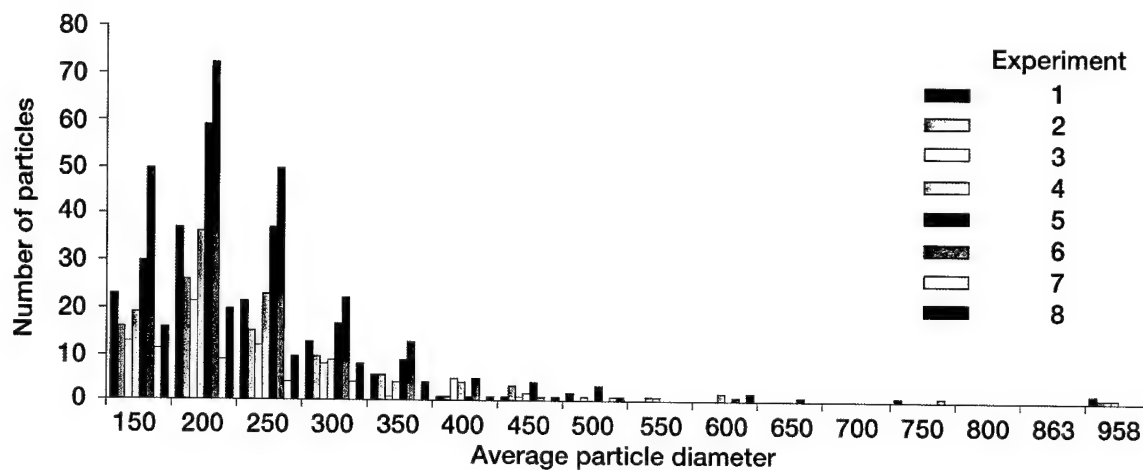


Figure 5.—Spur rig experiment after pitting damage was observed.

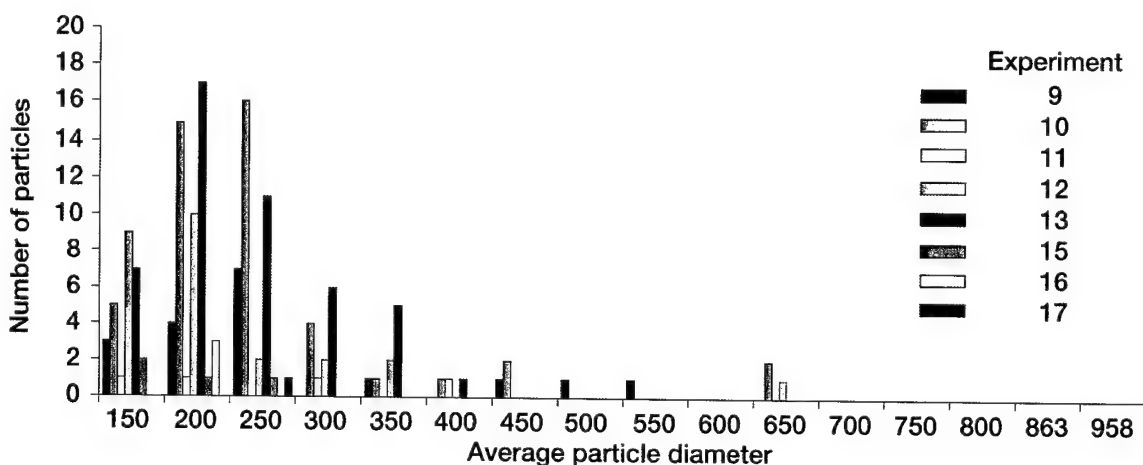


Figure 6.—Spur rig experiments with no damage.

Table 6.—Mean particle size for Spur Rig Experiments with Damage

Exp.	Rdg Prior to Damage	Mean Particle Size (μm)	Rdg With Damage	Mean Particle Size (μm)	Final Rdg with Damage	Mean Particle Size (μm)
1	10622	235	14369	249	15136	272
2	1573	236	2199	246	2444	272
3	N/A	N/A	2669	256	3029	254
4	518	252	2065	249	4863	254
5	N/A	N/A	2566	244	4425	234
6	9328	227	12061	229	12368	238
7	N/A	N/A	N/A	N/A	13716	230
8	N/A	N/A	5181	242	5314	268

Spiral Bevel Gear Test Rig

Six experiments, identified as Experiments 18 through 23, were performed with gear pitting damage in the Spiral Bevel Gear Fatigue Test Rig. Table 7 lists the total number of readings for each experiment and the amount of wear debris at test completion. Mean particle size was also calculated for the final reading for each experiment. Results of this calculation are also shown in Table 7. Pitting damage was observed on gear teeth on one pinion during all 6 experiments. In addition, bearing damage was observed during Experiment 18. This experiment resulted in the largest accumulated mass, but not the largest count value or the largest mean particle size.

Figures 7 and 8 are histograms of the number of particles for each average particle size diameter for Experiments 18 through 23.

Note only 14 particle size ranges were measured, as compared to 16 during Spur Rig experiments. Also note the smallest average particle diameter measured was 250 microns. Although the counts are higher than the counts measured during Spur Rig experiments, the distribution is also very similar to the spur rig experiments both with and without damage.

Table 7.—Spiral Bevel Rig Experiments with Pitting Damage

Exp.	Final Rdg	Mass (mg)	Counts	Mean Particle Size (μm)
18	4840	137.7	316	387
19	29495	42.0	283	306
20	N/A	104.3	341	365
21	1835	44.4	107	392
22	6073	26.5	104	329
23	10569	41.2	174	332

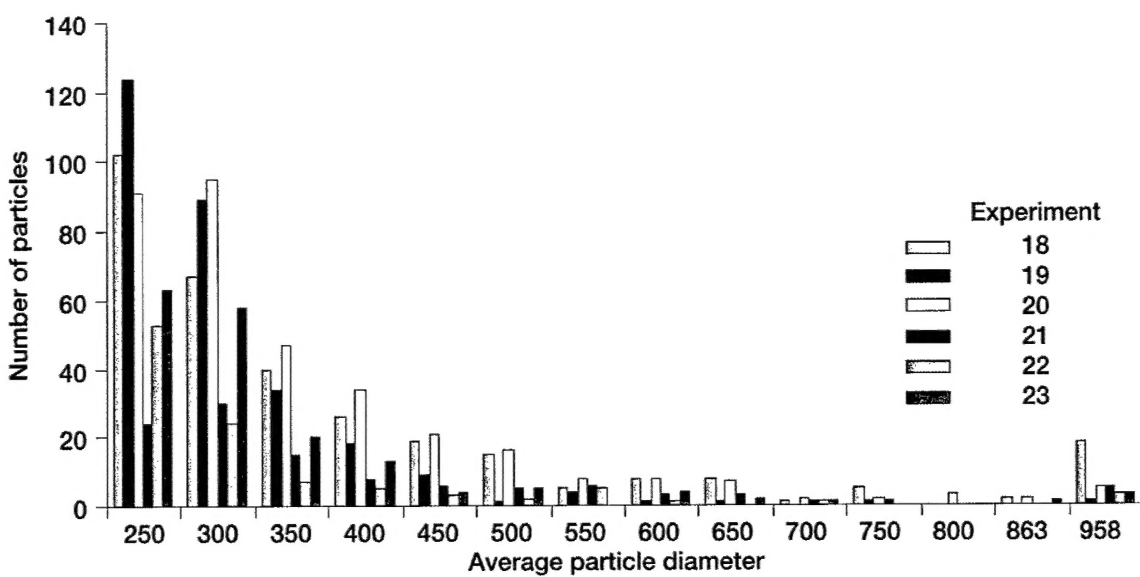


Figure 7.—Spiral bevel rig experiments with pitting damage.

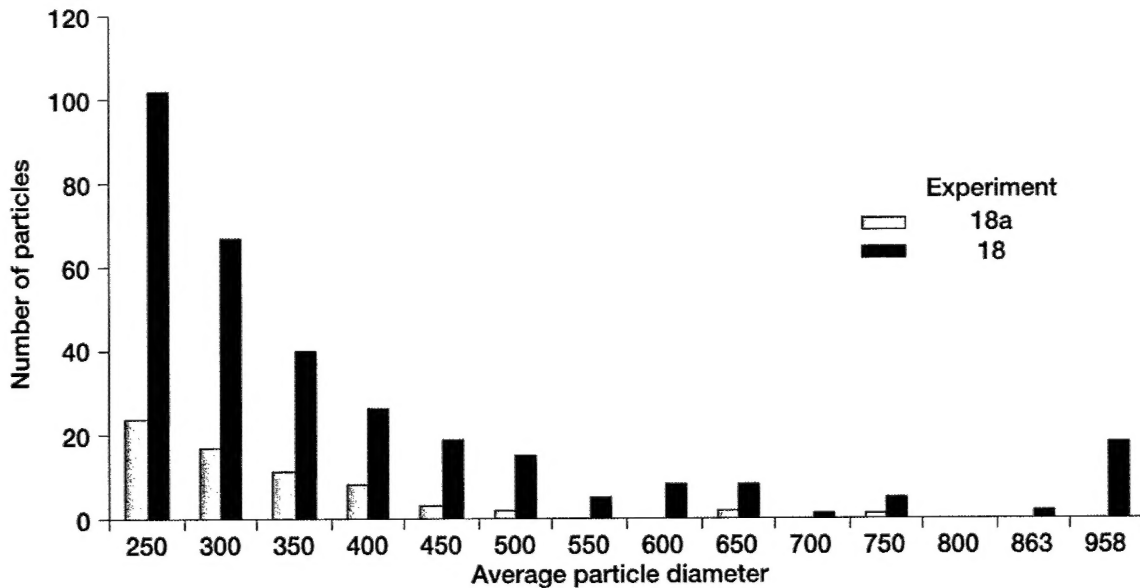


Figure 8.—Spiral bevel rig experiment with bearing failure.

Figure 9 is from the Spiral Bevel Rig Experiment 18 with both gear and bearing damage. The gears were inspected at reading 99 and initial pitting was beginning to occur on the right side of the test rig. The gears were inspected at test completion and destructive pitting to one tooth on the right side pinion was observed and is shown in Figure 2. At test completion, it was found that damage also occurred on the pinion bearing. This damage is also shown in Figure 2. It is believed that the pinion bearing initiated pitting damage at reading number 2592 due to the drastic change in accumulated mass from Figure 9. The legend label Exp. 18a in Figure 8, refers to the count data taken during Experiment 18 prior to bearing failure occurred, but pitting damage was observed on the pinion (Reading 2592). The counts increased significantly when bearing damage occurred, but the distribution is very similar to that of gear pitting damage particle distributions.

500-HP Helicopter Transmission Test Stand

Two experiments, identified as Experiments 24 and 25, were performed in the 500-hp Helicopter Transmission Test Stand. Table 8 lists the total number of readings for each experiment and the amount of wear debris at test completion. Mean particle size was also calculated for the final reading for each experiment. Results of this calculation are also shown in Table 8. As stated before, a spalled spiral-bevel gear duplex ball bearing was found at the end of Experiment 24. For Experiment 24, a large increase in debris occurred at reading number 2755. This also coincided with the test transmission chip detector indication of debris. After reading 2755, an exponential increase in accumulated debris occurred. At the end of the test, over half of the bearing inner race, over half of the outer race, and most of the balls were damaged (Figure 3c). Figure 10 is a histogram of average particle size for the end of Experiment 24.

For average particle diameters greater than 300mm, the distribution looks similar to the previous spur and spiral-bevel test rig results.

Table 8.—500hp Test Stand Experiments with Bearing Damage

Exp.	Final Rdg	Mass (mg)	Counts	Mean Particle Size (μm)
24	7965	635.6	2257	378
25	9503	35.2	188	338

Also as stated before, a spalled spiral-bevel pinion triplex ball bearing was found at the end of Experiment 25. A constant increase in debris occurred during this test. At the end of the test, a small portion of the outer bearing race was damaged (Figure 3d). Figure 11 is a histogram of average particle size for the end of Experiment 25. The distribution is similar to that of the spiral-bevel gear duplex ball bearing failure.

CONCLUSIONS

An oil debris diagnostic tool was evaluated for detecting fatigue damage to spur and spiral bevel gears and bearings from tests performed in the NASA Glenn Spur Gear Fatigue Rig, Spiral Bevel Gear Test Facility, and the 500hp Transmission Test Stand. Based on this analysis, the following conclusions can be made:

1. Oil debris alone cannot discriminate between bearing and gear fatigue damage when both share a common lubrication system.
2. Particle counts and oil debris mass increased with increase in damage magnitude.
3. Particle size distributions were very similar for normal wear or no damage conditions
4. Particle size distributions were very similar for gear pitting fatigue damage conditions and bearing pitting fatigue damage conditions.

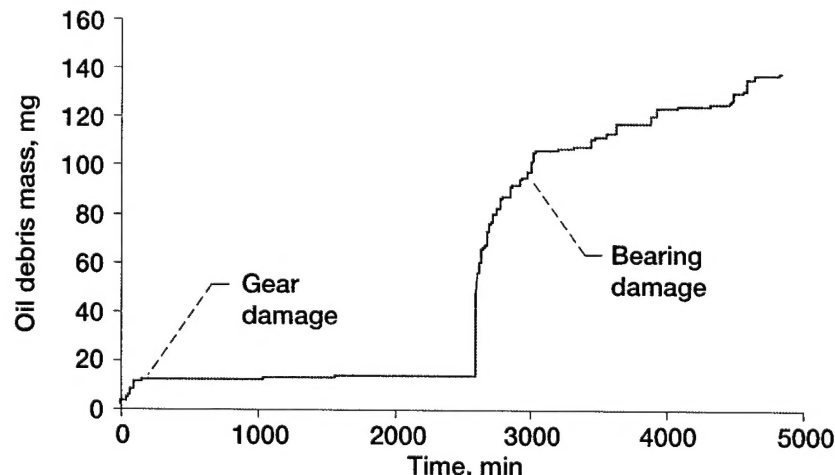


Figure 9.—Damage to right pinion gear and bearing during experiment 18.

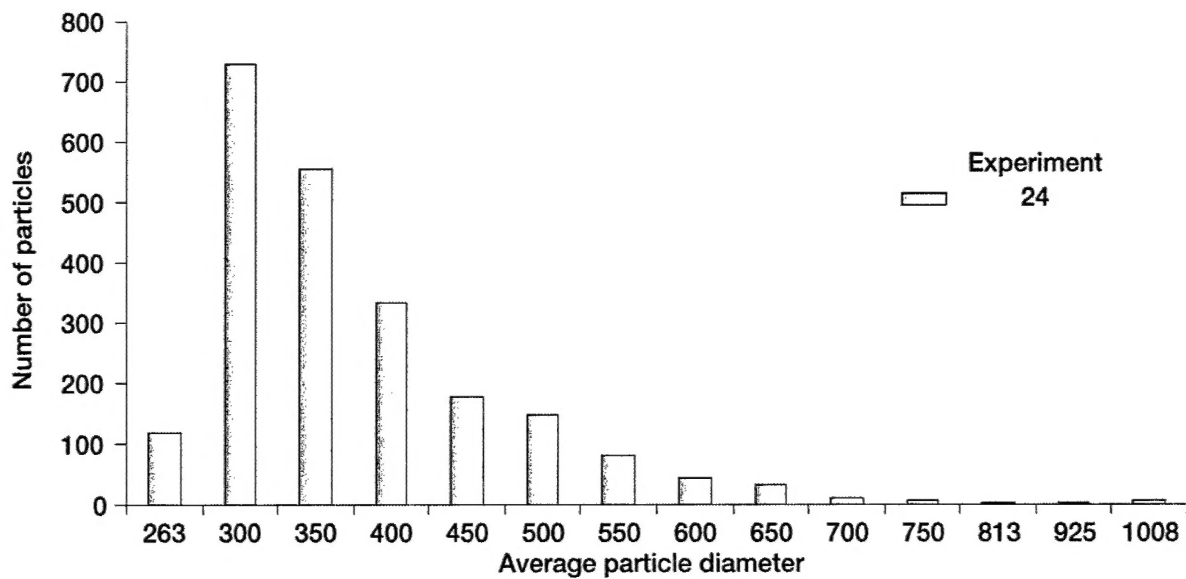


Figure 10.—500 hp test stand duplex bearing failure.

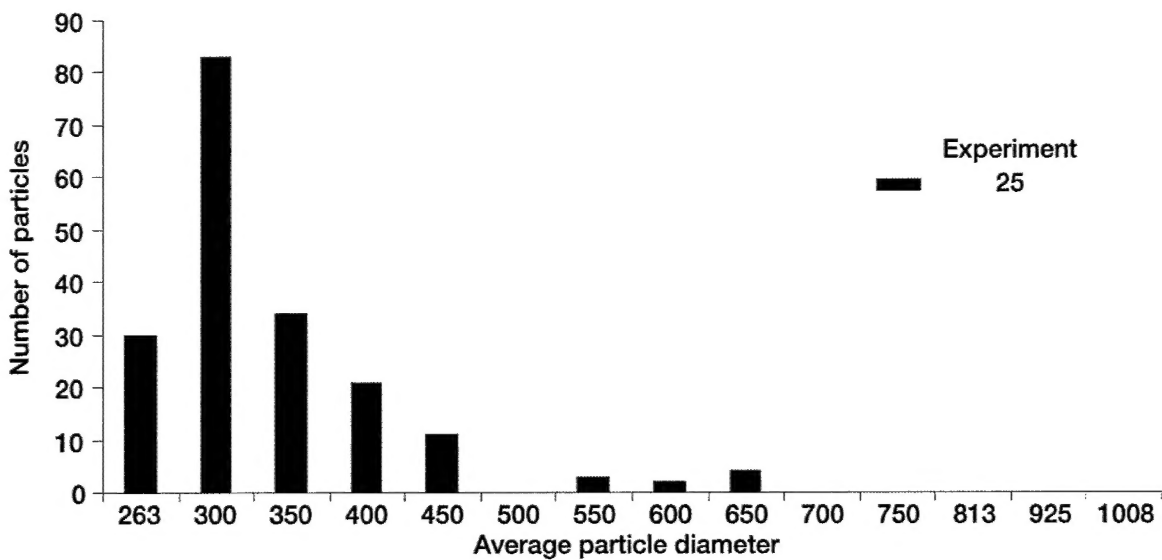


Figure 11.—500 hp test stand triplex bearing pinion failure.

REFERENCES

1. Larder, B.D., "Helicopter HUM/FDR: Benefits and Developments," American Helicopter Society 55th Annual Forum, Alexandria, VA, May 1999.
2. Stewart, R.M. and Ephraim, P., "Advanced HUMS and Vehicle Management Systems Implemented Through an IMA Architecture," American Helicopter Society 53rd Annual Forum, April 1997.
3. Pouradier, J. and Trouvé, M., "An Assessment of Eurocopter Experience in HUMS Development and Support," American Helicopter Society 57th Annual Forum, Alexandria, VA, May 2001.
4. Hunt, T.M., Handbook of Wear Debris Analysis and Particle Detection in Liquids, Elsevier Applied Science, London, United Kingdom, 1993.
5. Dempsey, P.J., "A Comparison of Vibration and Oil Debris Gear Damage Detection Methods Applied to Pitting Damage," NASA/TM—2000-210371, August 2000.
6. Dempsey, P.J., "Integrating Oil Debris and Vibration Measurements for Intelligent Machine Health Monitoring," PhD Thesis, The University of Toledo, May 2002.
7. Howe, B. and Muir, D., "In-Line Oil Debris Monitor (ODM) for Helicopter Gearbox Condition Assessment," AD-a347 503, Defense Technical Information Center, Ft. Belvoir, VA, July 1998.
8. Fisher, G. and Donahue, A., "Filter Debris Analysis as a First-Line Condition Monitoring Tool," Lubrication Engineering, February 2000.
9. Townsend, D.P., "Evaluation of the EHL Film Thickness and Extreme Pressure Additives on Gear Surface Fatigue Life," NASA/TM—1994-106663, July 1994.
10. Lynwander, P., "Gear Drive Systems: Design and Application," Marcel Dekker, New York, NY, 1983.
11. Townsend, D. P., Dudley's Gear Handbook, McGraw-Hill, New York, NY, 1991.
12. Handschuh, R. F., "Thermal Behavior of Spiral Bevel Gears," NASA/TM—1995-106518, January 1995.
13. Handschuh, R. F., "Testing of Face-Milled Spiral Bevel Gears at High-Speed and Load," NASA/TM—2001-210743.
14. Lewicki, D.G. and Coy, J.J., "Vibration Characteristics of OH-58A Helicopter Main Rotor Transmission," NASA/TP—1987-2705, April 1987.
15. Decker, H.D. and Lewicki, D.G., "Spiral Bevel Pinion Crack Detection in a Helicopter Gearbox," Proceedings of the 59th AHS Annual Forum, American Helicopter Society, Alexandria, VA, June 2003.
16. Roylance, B.J., "Monitoring Gear Wear Using Debris Analysis—Prospects for Establishing a Prognostic Method," 5th International Congress on Tribology, K. Holmberg and I. Nieminen, eds., Volume 4, pg. 85, June 1989.
17. Dempsey, P.J., "Gear Damage Detection Using Oil Debris Analysis," NASA/TM—2001-210936, September 2001
18. Dempsey, P.J., Handschuh, R.F., and Afjeh, A.A., "Spiral Bevel Gear Damage Detection Using Decision Fusion Analysis," NASA/TM—2002-211814, August 2002.